Bioorganic & Medicinal Chemistry Letters 24 (2014) 3772–3776

Contents lists available at ScienceDirect

Bioorganic & Medicinal Chemistry Letters

journal homepage: www.elsevier.com/locate/bmcl

Synthesis, characterization, antifungal evaluation and 3D-QSAR study of phenylhydrazine substituted tetronic acid derivatives

Ying Hu [a,c], Junjun Wang [b,c], Aimin Lu [a,b], Chunlong Yang [a,b,c,*]

[a] Jiangsu Key Laboratory of Pesticide Science, Nanjing Agricultural, Nanjing 210095, PR China
[b] Ministry of Agriculture, Key Laboratory of Monitoring and Management of Crop Diseases and Pest Insects, Nanjing Agricultural University, Nanjing 210095, PR China
[c] Department of Science, College of Science, Nanjing Agricultural University, Nanjing 210095, PR China

ARTICLE INFO

Article history:
Received 10 May 2014
Revised 23 June 2014
Accepted 25 June 2014
Available online 1 July 2014

Keywords:
Tetronic acid
Substituted phenylhydrazine
X-ray diffraction
Antifungal activity
3D-QSAR

ABSTRACT

A series of 3-(1-(2-(substituted phenyl)hydrazinyl)alkylidene)furan-2,4(3*H*,5*H*)-diones were designed and prepared using two synthetic routes. Their structures were confirmed by FT-IR, ^{1}H NMR, ^{13}C NMR, MS, elemental analysis and single-crystal X-ray diffraction. Their bioactivity was evaluated against *Botrytis cinerea* in vitro. Most target compounds exhibited remarkable antifungal activity. Two compounds **7f** and **7h** were highly effective and their EC_{50} values were 0.241 μg/mL and 0.167 μg/mL, respectively, close to that of the control drug procymidone. 3D-QSAR studies of CoMFA and CoMSIA were carried out. Models with good predictive ability were generated with the cross validated q^2 values for CoMFA and CoMSIA being 0.565 and 0.823. Conventional r^2 values were 0.983 and 0.945, respectively. The results provided a practical tool for guiding the design and synthesis of novel and more potent tetronic acid derivatives containing substituted phenylhydrazine moiety.

Much attention was paid to the isolation and synthesis of tetronic acid derivatives owing to the wide range of biological activities, such as antioxidant,[1,2] anti-HIV,[3] antiepileptic,[4,5] antitumor,[6] anti-inflammatory[7,8] and insecticidal[9,10] ones. Moreover, some of them exhibited high antimicrobial activities. 5-Hydroxyvertinolide and bislongiquinolide were isolated from the fungus *Trichoderma longibrachiatum* Rifai aggr., which were antagonistic to the fungus *Mycena citricolo*.[11] Based on pharmacophore hypothesis, substituted tetronic acid 3-carboxamides were investigated as inhibitors of undecaprenyl pyrophosphate synthase (UPPS) for use as novel antimicrobial agents.[12] Pestalotic acids A–G were new furylidene tetronic acid derivatives, isolated from a plant endophyte *Pestalotiopsis yunnanensis*, showed obvious antimicrobial activity.[13] Vitamin C palmitate was found to be an effective inhibitor of hyaluronan lyases from *Streptococcus pneumoniae* and *Streptococcus agalactiae* strain 4755.[14] 5-Spirotetronic acid derivatives containing ninhydrin residue showed good bacteriostatic activity against *Staphylococcus aureus* and *Escherichia coli*.[15]

In view of this, it is worth to develop new tetronic acid derivatives for screening high effective fungicides by modifying the substituents at furandione. In recent years, many compounds containing a moiety of substituted phenylhydrazine were found showing noticeable biological activity against the pathogenic fungi.[16–19] Based on active groups combination and bioisosterism principles, eleven substituted phenylhydrazine moieties were introduced at 3-position of furan-2,4(3*H*,5*H*)-dione, respectively to design and synthesize twenty-five novel tetronic acid derivatives, with a view to reveal the influence of introducing substituted phenylhydrazines on the fungicidal activity. In addition, CoMFA and CoMSIA implemented in the SYBYL software packages were used to develop predictive 3D-QSAR models.[20–23] This study also predicted the substituents of new tetronic acid derivatives with potential antifungal activities based on 3D-QSAR analysis.

The intermediate **3** was prepared by the reported method,[24] starting from L-ethyl lactate, through β-ketoacylation of the hydroxyl and cyclization by lactonization and acidification (Scheme 1). The cyclization was so-called Lacey–Dieckmann condensation. The key to the lactonization reaction was the choice of an appropriate base. According to the known procedure, various bases have so far been employed to realize the lactonization.[25,26] In this article, CH_3ONa/CH_3OH, Na/Toluene and *t*-BuOK/THF were studied comparatively. All the bases with 1.2 equiv were in anhydrous form. According to the results summarized in Table 1, the reaction proceeded readily in *t*-BuOK/THF at reflux, leading to the expected intermediate **3** in 71.0% yield after 12 h. In the same reaction time, this yield of entry 3 was apparently higher than 20.3% of entry 2. Moreover, TLC (ethyl acetate/light petroleum/methanol/acetic acid, v/v, 10:2:2:0.2) showed the complex oil obtained from entry 1 contained the intermediate **3**, but it was difficult to be isolated.

* Corresponding author. Tel.: +86 25 8439 5207.
E-mail address: ycl@njau.edu.cn (C. Yang).

http://dx.doi.org/10.1016/j.bmcl.2014.06.074
0960-894X/

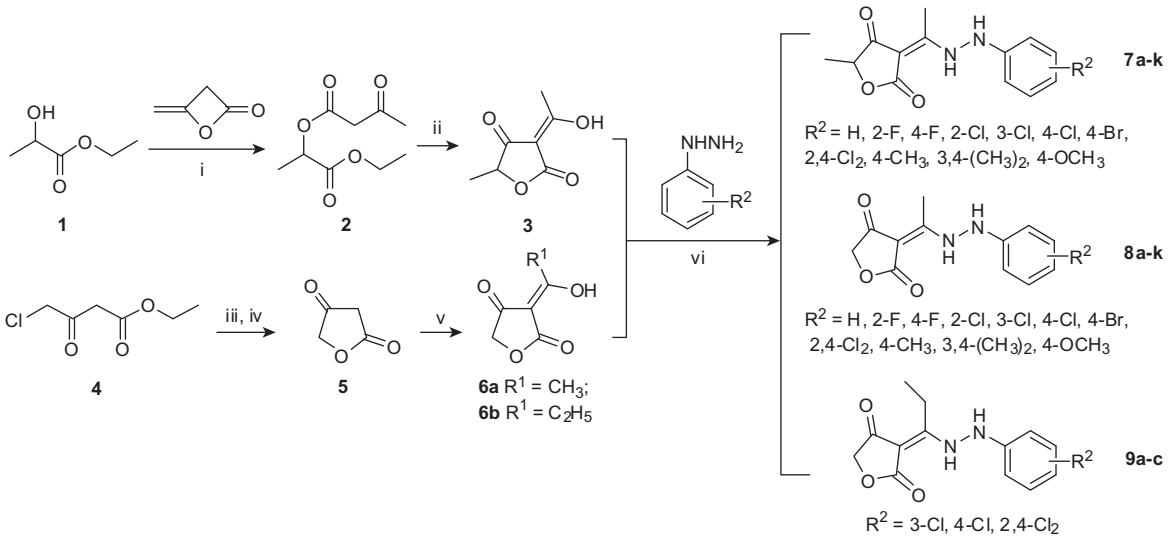

Scheme 1. Reagents and conditions: (i) CH_3OH, −10 °C to rt, 12 h (82%); (ii) *t*-BuOK/THF, reflux, 20% HCl (71%); (iii) *t*-BuOK/THF, rt, 20 h, 5% HCl (95%); (iv) acetic acid, HCl gas, 1 h (69%); (v) acyl chloride/DMAP/CH_2Cl_2, −15 °C to rt, 15 h; (vi) ethanol, rt, 3–6 h.

Table 1
The optimization of preparation of the intermediates **3** and **6a**

Entry	Compd	Base	Solvent	Temp.	Yield (%)
1	**3**	CH_3ONa	Methanol	Reflux	10.7
2	**3**	Na	Toluene	rt	20.3
3	**3**	*t*-BuOK	THF	Reflux	71.0
4	**6a**	CH_3ONa	Methanol	Reflux	2.6
5	**6a**	Na	Toluene	rt	4.9
6	**6a**	*t*-BuOK	THF	Reflux	9.5

The intermediates **6a–b** were tried to be prepared with the same methods, but the experiments showed that all the yields in three conditions were very low, even in *t*-BuOK/THF. So the intermediates **6a–b** were tried to be synthesized in another route, starting from 4-chloroacetoacetate, through oxyalkylation, cyclization and the acetylation at 3-position of furan-2,4(3*H*,5*H*)-dione.[27,28] The result indicated that the total yields of **6a–b** amounted up to 31.4% and 30.7%, respectively.

The synthesis of the target compounds **7a–k**, **8a–k**, **9a–c** were performed by the reaction of **3** and **6a–b** with eleven substituted phenylhydrazines respectively in ethanol at room temperature. The reaction was gentle and the progress was monitored by TLC (ethyl acetate/light petroleum/methanol/acetic acid, v/v, 10:2:2:0.2). The yields of the target compounds ranged from 32.7% to 51.1% (Table 2). Each target compound was found containing the *cis–trans*-isomers, which was caused by the double bond at 3-position of furan-2,4(3*H*,5*H*)-dione.

Table 2
Products and the corresponding yields

Compd	R^2	Yield (%)	Compd	R^2	Yield (%)
7a	H	47.5	**8c**	4-F	49.1
7b	2-F	37.5	**8d**	2-Cl	47.1
7c	4-F	45.6	**8e**	3-Cl	40.1
7d	2-Cl	51.1	**8f**	4-Cl	48.9
7e	3-Cl	36.2	**8g**	4-Br	38.9
7f	4-Cl	43.7	**8h**	2,4-Cl_2	40.3
7g	4-Br	48.3	**8i**	4-CH_3	50.3
7h	2,4-Cl_2	43.9	**8j**	3,4-$(CH_3)_2$	43.9
7i	4-CH_3	49.1	**8k**	4-OCH_3	45.9
7j	3,4-$(CH_3)_2$	42.4	**9a**	3-Cl	41.2
7k	4-OCH_3	43.1	**9b**	4-Cl	50.0
8a	H	42.7	**9c**	2,4-Cl_2	38.2
8b	2-F	32.7			

The isomers of target compounds could be observed by ^{1}H NMR and ^{13}C NMR spectrums. The signals for the protons of NH close to five-membered ring in ^{1}H NMR spectra and almost all the signals for carbon atoms of furan ring and olefinic carbons in the ^{13}C NMR spectra were divided into two single peaks, which was the proof of the existence of *cis–trans*-isomers.

As displayed in Figure 1, the single-crystal X-ray diffraction study of compound **8a** also suggested the existence of *cis–trans*-isomerism. The suitable crystal was obtained by slow evaporation of the solution composed of acetone and petroleum ether at room temperature. The compound **8a** crystallized with two independent molecules (Molecule A and B) in the asymmetric unit. In the Molecule A, the intramolecular hydrogen bond N1–H1···O3 (Fig. 1), together with the atoms C3, C2 and C5, formed a new six-membered ring. The bond lengths of N1–C5 [1.323(3) Å], N2–C7 [1.407(3) Å], C1–C2 [1.454(3) Å] and C2–C3 [1.409(3) Å] were shorter than their normal bond lengths because of the presence of an electronic delocalization. Molecule B was

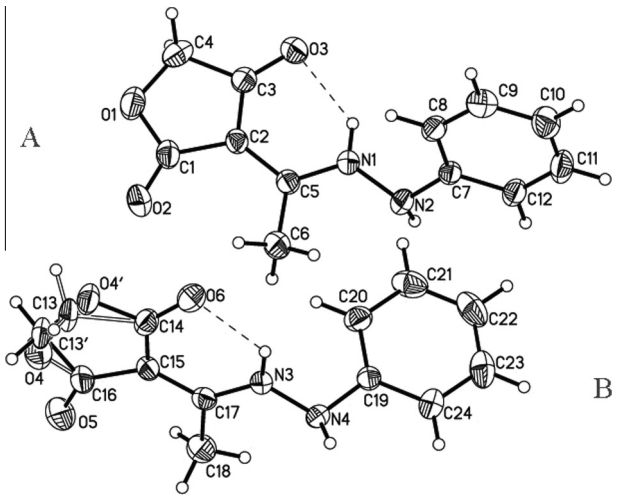

Figure 1. The X-ray crystal structure of compound **8a**, shown with 50% probability displacement ellipsoid.

similar to Molecule A. The difference between Molecule A and B was that Molecule B was a *cis–trans*-isomer due to the disordered state of O4 and C13, while Molecule A was a *trans*-isomer.

Gaussian 03W software was used to decide the most stable conformer of the compounds.[29] The *trans*-isomer α and *cis*-isomer β were shown in Figure 2. The compounds **7f** and **8a** were chosen as the models for calculation. The HF/3-21G was used for preliminary optimization, and B3LYP/6-31G* was applied for further optimization. Single point energies of two compounds were calculated with DFT method at B3LYP/6-311++G** level. The solvent effect of DMSO was also taken in account. The calculated results showed that the relative energies of **7f**α and **7f**β were 0.00 and 1.44 kJ/mol, while those of **8a**α and **8a**β were 0.00 and 1.07 kJ/mol. It should be speculated that *trans*-isomer was predominant. This was consistent with the result of the X-ray diffraction study. The ratios of *trans*-isomer were estimated at 55–60% according to the intensities of the two pairs of peaks in the NMR spectrum.

All the target compounds were screened for antifungal activity against *Botrytis cinerea*.[30] The fungicide procymidone was used as control drug. Procymidone and iprodione are the general fungicides against *B. cinerea*. The reports gave the corresponding EC_{50} values of 0.32 μg/mL and 0.80 μg/mL, respectively.[31,32] These data demonstrated the potential application value of the high active title compounds. The results in Table 4 showed that most target compounds exhibited remarkable fungicidal activity. Among them, the compounds **7f–h** and **8g** were highly effective against *B. cinerea* and their EC_{50} values were 0.241 μg/mL, 0.283 μg/mL, 0.167 μg/mL and 0.294 μg/mL, respectively, close to or lower than 0.240 μg/mL of the control drug.

To analyze the structure–activity relationship, the CoMFA and CoMSIA 3D-QSAR models with a total of twenty-five target compounds were developed.[33,34] The statistical parameters were given in Table 3. The CoMFA model (q^2 = 0.565, r^2 = 0.983) was based on the steric and electrostatic fields, and the CoMSIA model (q^2 = 0.823, r^2 = 0.945) was based on the steric, electrostatic, hydrophobic, hydrogen bond donor and hydrogen bond acceptor fields. Partial least-square (PLS) analysis was performed to establish a linear relationship between the molecular fields and the activity of molecules. Figure 3 showed the alignment of all target compounds used in the training set. Contour maps for the CoMFA and CoMSIA models were displayed in Figure 4. Experimental and predicted pEC_{50} values for the training set and test set were reported in Table 4, and the correlation plots of CoMFA and CoMSIA models were shown in Figures. 5 and 6, respectively.

Steric CoMFA map (Fig. 4A) showed green contour around 4-position of phenyl ring indicating bulky groups were favored at this position. It was confirmed that the compounds **7f–h**, **8f–h** and **9b–c** exhibited higher antifungal activity. The yellow contours around 3-position of phenyl ring indicated that compounds with bulky groups at this position were less potent. This explained that the compounds **7e**, **8e** and **9a** had not good fungicidal activity.

Electrostatic CoMFA contour map (Fig. 4B) was shown in red around 4-position of phenyl ring indicating that negative charge might play a favorable role on activity, such as the compounds **7f–h**, **8f–h**, **9b–c**. Combined with the steric CoMFA map, the bulky groups with negative charges were favored at 4-position of phenyl ring. That also explained that the compounds **7c** and **8c** had worse fungicidal activity than **7f** and **8f**, respectively, due to the smaller atom radius of fluorine. The blue contours around almost whole phenyl ring showed that electronegative atom was disfavored at other positions except for 4-position. The compounds **7b**, **7d–e**, **8b** and **8d–e** were good examples.

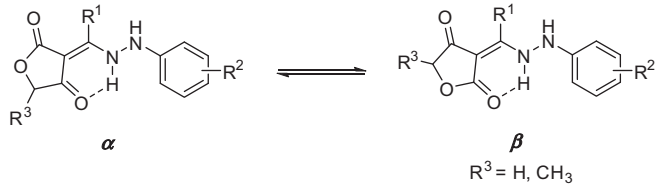

Figure 2. The *cis–trans*-isomers of target compounds.

Table 3
PLS statistics of CoMFA and CoMSIA 3D-QSAR models

PLS statistics	CoMFA	CoMSIA
q^2[a]	0.565	0.823
r^2[b]	0.983	0.945
s[c]	0.090	0.151
F[d]	180.464	103.152
ONC[e]	5	3
Steric[f]	0.498	0.164
Electrostatic[g]	0.502	0.330
Donor[h]		0.024
Acceptor[h]		0.024
Hydrophobic[i]		0.458

[a] Cross-validated correlation coefficient from leave-one-out.
[b] Noncross-validated r^2.
[c] Standard error of estimate.
[d] F-test value.
[e] Optimum number of principal components.
[f] Steric field contribution.
[g] Electrostatic field contribution.
[h] Donor and acceptor, of hydrogen bond fields contribution, respectively.
[i] Hydrophobic field contribution.

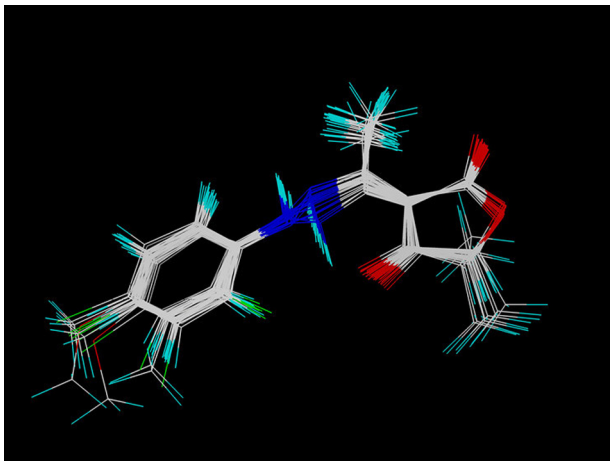

Figure 3. Alignment of all target compounds in the training set.

The colors of the steric and electrostatic contour maps in the CoMSIA model had the same meanings as those of the CoMFA model. Similar to steric CoMFA map, steric CoMSIA contour map (Fig. 4C) indicated bulky group was favored at 4-position of phenyl ring. In addition, the green contour around 5-position of furandione nucleus suggested that bulky group should be introduced at this position. So the compounds **7** showed better bioactivity than the compounds **8**, roughly. In agreement with CoMFA model, electrostatic CoMSIA map (Fig. 4D) indicated that the group with negative charge was also favored at 4-position of phenyl ring.

Hydrophobic CoMSIA contour map (Fig. 4E) showed yellow contour around 4-position of phenyl ring indicating that hydrophobic group was favored at the position, such as the compounds **7f–h**, **8f–h** and **9b–c**. The grey contours around 2- and 3-position of phenyl ring indicated that hydrophobic group played a disfavored role at these positions. The compounds **7b**, **7d–e**, **8b** and **8d–e** were good examples.

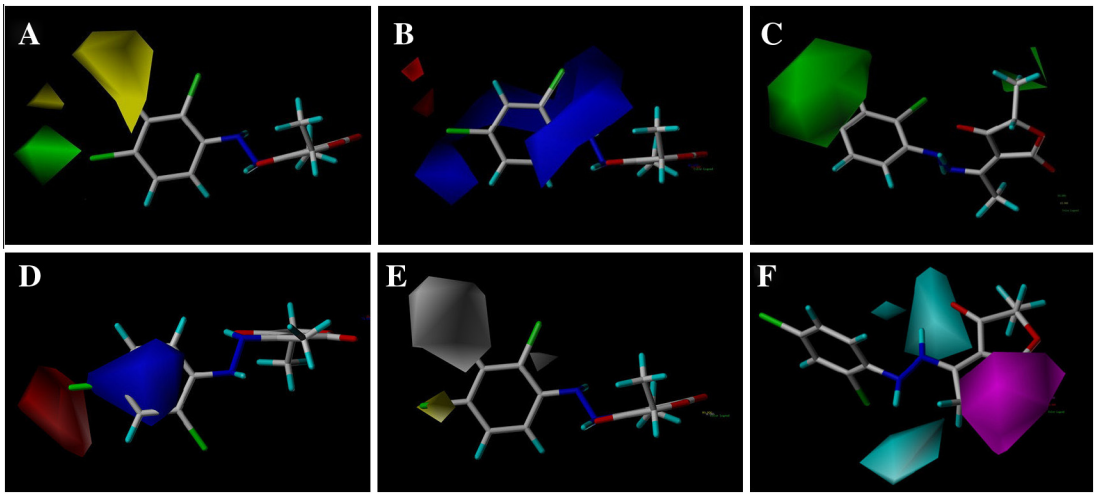

Figure 4. CoMFA and CoMSIA STDEV*COEFF contour maps. CoMFA model: (A) Sterically favored areas are in green, and sterically disfavored areas are in yellow. (B) Negative charge favored areas are in red and disfavored areas are in blue. CoMSIA model: The colors in (C) and (D) have the same meanings as do CoMFA contour maps (A) and (B), respectively. (E) Hydrophobic favored areas are in yellow and disfavored areas are in gray. (F) Donor and acceptor favored areas are in cyan and magenta, respectively, and donor and acceptor disfavored areas are in purple and red, respectively.

Table 4
Experimental and predicted pEC_{50} values of compounds **7a–k**, **8a–k** and **9a–c** (μg/mL)

Compd	Actual EC_{50}	Actual pEC_{50}[b]	CoMFA		CoMSIA	
			Predicted pEC_{50}[b]	Residual	Predicted pEC_{50}[b]	Residual
7a	3.902	5.409	5.397	0.0122	5.440	−0.0311
7b	1.467	5.833	5.762	0.0718	5.806	0.0275
7c	1.139	5.943	5.919	0.0243	6.133	−0.1892
7d	1.586	5.800	5.716	0.0840	5.787	0.0128
7e	1.350	5.870	5.807	0.0629	5.901	−0.0315
7f	0.241	6.619	6.652	−0.0333	6.508	0.1105
7g	0.283	6.548	6.501	0.0470	6.527	0.0211
7h	0.167	6.777	6.768	0.0083	6.767	0.0100
7i	2.270	5.644	5.512	0.1316	5.313	0.3305
7j	18.743	4.727	4.902	−0.1748	5.018	−0.2906
7k	13.951	4.855	4.906	−0.0508	4.891	−0.0358
8a	3.997	5.398	5.538	−0.1393	5.644	−0.2458
8b	1.045	5.981	5.916	0.0652	6.101	−0.1206
8c	0.585	6.233	6.288	−0.0548	6.244	−0.0109
8d	1.801	5.744	5.790	−0.0461	5.765	−0.0209
8e	1.060	5.975	5.993	−0.0186	5.791	0.1832
8f	0.337	6.472	6.467	0.0045	6.410	0.0617
8g	0.294	6.531	6.499	0.0322	6.592	−0.0605
8h	0.305	6.515	6.625	−0.1097	6.515	0.0004
8i	2.325	5.633	5.700	−0.0668	5.430	0.2031
8j	7.904	5.102	5.009	0.0936	5.041	0.0615
8k	9.664	5.015	4.958	0.0564	5.000	0.0148
9a[a]	1.549	5.810	6.054	−0.2440	5.751	0.0590
9b[a]	0.360	6.443	6.530	−0.0870	6.460	−0.0170
9c[a]	0.517	6.286	6.759	−0.4730	6.698	−0.4120
Procymidone	0.240	—	—	—	—	—

[a] Compounds in the test set.
[b] $pEC_{50} = -\log(EC_{50})$.

Donor and Acceptor CoMSIA contour maps (Fig. 4F) showed that magenta contour around 2-position of furandione nucleus suggested that hydrogen bond acceptor was favored at this area. While cyan contours around NH of hydrazine and 2-position of phenyl ring indicated that hydrogen bond donor was favored. Among them, *ortho*-substitution of phenyl ring was worthy for further discussion. The relation between *ortho*-substitution and bioactivity depended on many factors. In this model, hydrogen bond was not the key factor (donor field contribution was 0.024). So the introduction of halogen atom at 2-position of phenyl ring could improve the activity not largely, such as the compounds **7b**, **7d**, **8b** and **8d**, but slightly. This could be used to explain that compounds **7h** and **8h** had little better activity than compounds **7f** and **8f**, respectively.

The analysis of contour maps for CoMFA and CoMSIA models indicated that the introduction of bulky group with negative charge at 4-position of phenyl ring could largely improve the fungicidal activity. And bulky groups at 2- and 3-position of phenyl ring played an unfavorable role in bioactivity. The substitution at 5-position of furandione nucleus with methyl was favored in the current data set. Moreover, carbonyl group at 2-position of furandione nucleus could generate an area with negative charge that

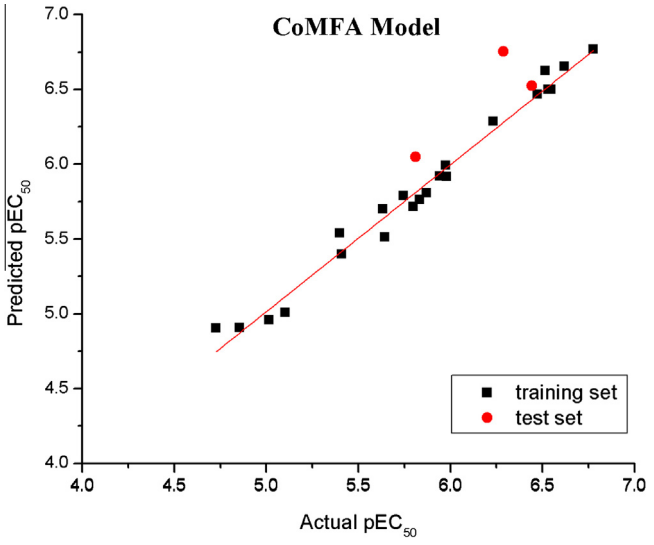

Figure 5. Plot of actual and predicted activities for training set and test set based on CoMFA model.

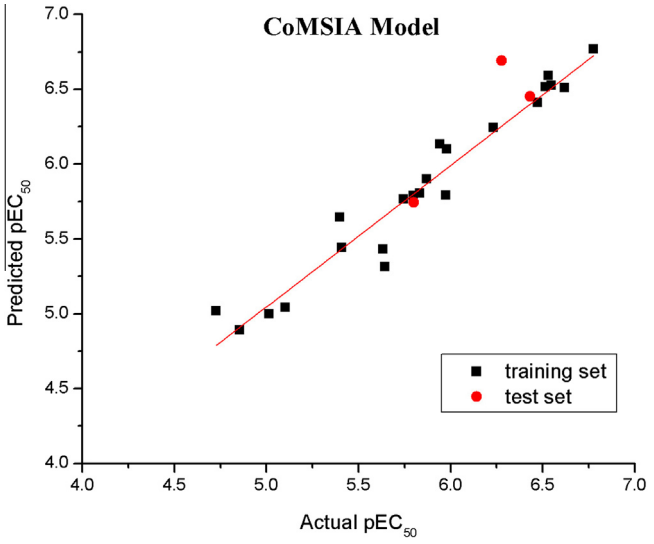

Figure 6. Plot of actual predicted activities for training set and test set based on CoMSIA model.

could act as hydrogen bond acceptor, and the amino group of hydrazine could generate areas with positive charges that could act as hydrogen bond donors involving the binding site.

In conclusion, the substituted phenylhydrazine moieties were introduced at 3-position of furan-2,4(3*H*,5*H*)-dione to design and synthesize a series of novel tetronic acid derivatives. The structures of these compounds were well supported by spectroscopic data, elemental analysis and single-crystal X-ray diffraction analysis. The bioassay results indicated that most target compounds showed remarkable fungicidal activity against *B. cinerea*. Two compounds **7f** and **7h** were highly effective, their EC_{50} values were near to the control drug procymidone. CoMFA and CoMSIA 3D-QSAR models were generated and showed good q^2 and r^2 values. These models provided a practical tool for the modification and optimization of the structures of tetronic acid derivatives containing substituted phenylhydrazine moiety to further improve the antifungal activity.

Acknowledgments

The authors gratefully acknowledge the financial support of the National Key Technologies R&D Program of China (No. 2011 BAE06B04).

Supplementary data

Supplementary data (The crystallographic data for the structure analysis of the compound **8a** has been deposited with the Cambridge Crystallographic Data Center, CCDC No. 981945. Copies of this information can be obtained free of charge from the Director, CCDC, 12 Union Road, Cambridge, CB2 1EZ, UK (fax: +44 1223 336 033; or E-mail: deposit@ccdc.cam.ac.uk or URL: http://www.ccdc.cam.ac.uk).) associated with this article can be found, in the online version, at http://dx.doi.org/10.1016/j.bmcl.2014.06.074.

References and notes

1. Schobert, R.; Schlenk, A. *Bioorg. Med. Chem.* **2008**, *16*, 4203.
2. El-Gendy, K. S.; Aly, N. M.; Mahmoud, F. H.; Kenawy, A.; El-Sebae, A. K. H. *Food Chem. Toxicol.* **2010**, *48*, 215.
3. Roggo, B. E.; Petersen, F.; Delmendo, R.; Jenny, H. B.; Peter, H. H.; Roesel, J. *J. Antibiot.* **1994**, *47*, 136.
4. Zhang, C. L.; Chatterjee, S. S.; Stein, U. N.-S. *Arch. Pharmacol.* **1992**, *345*, 85.
5. Willmore, L. J. *Curr. Opin. Invest. Drug* **2001**, *2*, 1763.
6. Hamaguchi, T.; Sudo, T.; Osada, H. *FEBS Lett.* **1995**, *372*, 54.
7. Foden, F. R.; McCormick, J.; O'Mant, D. M. *J. Med. Chem.* **1975**, *18*, 199.
8. Weber, V.; Rubat, C.; Duroux, E.; Lartigue, C.; Madesclaire, M.; Coudert, P. *Bioorg. Med. Chem.* **2005**, *13*, 4552.
9. Zhao, J. H.; Ji, M. H.; Xu, X. H.; Cheng, J. L.; Zhu, G. N. *Chin. Chem. Lett.* **2009**, *20*, 1307.
10. Zhao, J. H.; Zhou, Y.; Xu, X. H.; Cheng, J. L.; Zhu, G. N. *Chin. J. Struct. Chem.* **2009**, *28*, 837.
11. Andrade, R.; Ayer, W. A.; Trifonov, L. S. *Aust. J. Chem.* **1997**, *50*, 255.
12. Peukert, S.; Sun, Y. C.; Zhang, R.; Hurley, B.; Sabio, M.; Shen, X. Y.; Gray, C.; Dzink-Fox, J.; Tao, J.; Cebula, R.; Wattanasin, S. *Bioorg. Med. Chem. Lett.* **2008**, *18*, 1840.
13. Zhang, F.; Ding, G.; Li, L.; Cai, X. Y.; Si, Y. K.; Guo, L. D.; Che, Y. S. *Org. Biomol. Chem.* **2012**, *10*, 5307.
14. Spickenreither, M.; Braun, S.; Bernhardt, G.; Dove, S.; Buschauer, A. *Bioorg. Med. Chem. Lett.* **2006**, *16*, 5313.
15. Gein, V. L.; Gein, L. F.; Sheptukha, M. A.; Voronina, É. V. *Pharm. Chem. J.* **2005**, *39*, 537.
16. Yan, T.; Yu, S. J.; Liu, P. F.; Liu, Z.; Wang, B. L.; Xiong, L. X.; Li, Z. M. *Chin. J. Chem.* **2012**, *30*, 919.
17. Chee, G. L.; Dekeyser, M. A.; Seebold, K. W. J.; Osika, E. M.; Brouwer, W. G. U.S. Patent 4,016,324, 2005; *Chem. Abstr.* **2005**, *142*, 93517.
18. Hamid, A.; Sadiq, Z.; Yaqub, G.; Khan, N.; Iqbal, S.; Iqbal, K.; Ijaz, Z.; Bajwa, A. *J. Asian Chem.* **2013**, *25*, 5412.
19. Zou, M.; Lu, J. R.; Xin, C. W.; Bao, X. R.; Zhu, S. S.; Liu, Q.; Li, J. T.; Qiu, J. B. *J. Tianjin Univ. Technol.* **2010**, *26*, 1.
20. Li, R. L. *Drug structure–activity relationship*; China Pharmaceutical Technology: Beijing, 2004; pp 419–513. vol. 2.
21. Cramer, R. D.; Patterson, D. E.; Bunce, J. D. *J. Am. Chem. Soc.* **1988**, *110*, 5959.
22. Klebe, G.; Abraham, U.; Mietzner, T. *J. Med. Chem.* **1994**, *37*, 4130.
23. Rao, G. W.; Wang, C.; Wang, J.; Zhao, Z. G.; Hu, W. X. *Bioorg. Med. Chem. Lett.* **2013**, *23*, 6474.
24. Lacey, R. N. *J. Chem. Soc.* **1954**, 832.
25. Yuki, H.; Tsujimoto, T.; Sawada, T.; Takiura, K.; Yamaguchi, T. *Yakugaku Zasshi* **1976**, *96*, 536.
26. Mallinger, A.; Gall, T. L.; Mioskowski, C. *Synlett* **2008**, 386.
27. Kouhei, F.; Mitsuru, O. E. P. Patent 2,163,549, 2010; *Chem. Abstr.* **2010**, *152*, 357780.
28. Nomura, K.; Hori, K.; Arai, M.; Yoshii, E. *Chem. Pharm. Bull.* **1986**, *34*, 5188.
29. Skylaris, C.-K.; Igglessi-Markopoulou, O.; Detsi, A.; Markopoulos, J. *Chem. Phys.* **2003**, *293*, 355.
30. Wang, X. F.; Si, T. F.; Li, Q. B.; Zhu, Z. Y.; Zhu, X. J.; Qiang, S.; Yang, C. L. *ARKIVOC* **2010**, *ii*, 31.
31. Leroux, P.; Walker, A. S. *Eur. J. Plant Pathol.* **2013**, *135*, 683.
32. Zhang, C. Y.; Gao, Z. M.; Yue, Y. D. *Pesticide* **2003**, *42*, 28.
33. Yang, C.; Shao, Y. H.; Zhi, X. Y.; Huan, Q.; Yu, X.; Yao, X. J.; Xu, H. *Bioorg. Med. Chem. Lett.* **2013**, *23*, 4806.
34. Gupte, A.; Buolamwini, J. K. *Bioorg. Med. Chem. Lett.* **2009**, *19*, 314.